

momenta on the lower propagator lines. For the case of time-reversal invariance we thus have the relation between the twisted ladder diagrams and the Diffuson:

$$C_{\mathbf{p},\mathbf{p}'}(\mathbf{q},\omega) = D_{(\mathbf{p}-\mathbf{p}'+\mathbf{q})/2,(\mathbf{p}'-\mathbf{p}+\mathbf{q})/2}^{(\mathbf{p}+\mathbf{p}',\omega)} \quad (8.178)$$

In section 8.7 we calculated the Diffuson for small momentum difference (between upper and lower line momentum input values) and we therefore obtain for the twisted ladder diagrams for small total momentum

$$C_{\mathbf{p},\mathbf{p}'}(\mathbf{q},\omega) = \frac{u^2/\tau}{-i\omega + D_0(\mathbf{p} + \mathbf{p}')^2\hbar^{-2}} \quad (8.179)$$

where the last equality is valid in the momentum regime, $|\mathbf{p} + \mathbf{p}'|l \ll \hbar$, and $\omega\tau \ll 1$, $q \ll k_F$.

In the case of time-reversal invariance, we can thus relate a singular behavior of one class of diagrams to a singularity in different variables in another set of diagrams. In the next chapter this property will be exploited to classify all four-point diagrams, and diagrammatically derive the self-consistent theory of localization.

Chapter 9

Localization

In this chapter the quantum mechanical motion of a particle in a random potential at zero temperature is addressed. After presenting the scaling theory of localization, and verifying its predictions in the weak-disorder regime, the self-consistent theory of localization is presented.

In a seminal paper of 1958, P. W. Anderson showed that a particle's motion in a sufficiently disordered three-dimensional system behaves quite differently from that predicted by classical physics according to the Boltzmann theory [35]. In fact, at zero temperature diffusion will be absent, as particle states are localized in space due to the random potential. A sufficiently disordered system therefore behaves as an insulator and not as a conductor! By changing the impurity concentration, a transition from metallic to insulating behavior occurs. This is called the Anderson metal-insulator transition. In this chapter we shall discuss the phenomenon of Anderson localization using the developed diagrammatic technique.

In a pure metal, the Bloch or plane wave eigenstates of the Hamiltonian are current carrying

$$\langle \hat{\mathbf{j}} \rangle_{ext} = \int d\mathbf{x} \langle \mathbf{p} | \hat{\mathbf{j}}(\mathbf{x}) | \mathbf{p} \rangle = e \mathbf{v}_{\mathbf{p}}. \quad (9.1)$$

In a sufficiently disordered system, a typical eigenstate has a finite extension, and does not carry any current

$$\langle \hat{\mathbf{j}} \rangle_{loc} = \mathbf{0}. \quad (9.2)$$

The last statement is not easily made rigorous, and the phenomenon of localization is quite subtle. We shall return to the discussion of wave function localization in section 9.3.3.

Astonishing progress in the understanding of transport in disordered systems has taken place since the introduction of the scaling theory of localization [38]. A key ingredient in the subsequent development of the understanding of the transport properties of disordered systems was the intuition provided by diagrammatic perturbation theory. We shall exploit this in the present chapter, as well as in chapter 11 where we will discuss the weak localization effect. We start by considering the scaling theory.¹

¹The scaling theory of localization has its inspiration in the seminal work of Wegner [36] and

9.1 Scaling Theory of Localization

We shall consider a macroscopically homogeneous conductor, i.e., one with a spatially uniform impurity concentration. We consider that the temperature is zero. The conductance, the inverse resistance, of a d -dimensional macroscopically homogeneous hypercube of linear dimension L is according to eq.(8.74) proportional to the conductivity²

$$G(L) = \sigma L^{d-2}. \quad (9.3)$$

The conductance has dimension of e^2/\hbar , independent of the spatial dimension of the sample. In the following, the dimensionless conductance of a hypercube, defined as

$$g(L) \equiv \frac{G(L)}{\frac{e^2}{\hbar}} \quad (9.4)$$

will be of importance.

The one-parameter scaling theory of localization is based on the assumption that the dimensionless conductance solely determines the conductivity behavior of a disordered system. Consider fitting n^d identical blocks of length L (i.e., having the same impurity concentration, and with mean free paths smaller than the size of the system, $l < L$) into a hypercube of linear dimension nL . The conductance of the hypercube $g(nL)$ is then related to the conductance of each block $g(L)$ by

$$g(nL) = f(n, g(L)) \quad (9.5)$$

This is the one-parameter scaling assumption, the conductance of each block solely determines the conductance of the larger block, there is no extra dependence on microscopic parameters (such as l or λ_F).

For a continuous variation of the linear dimension of a system, the one-parameter scaling assumption results in the logarithmic derivative being solely a function of the dimensional conductance

$$\frac{d \ln g}{d \ln L} = \beta(g). \quad (9.6)$$

This can be seen by differentiating eq.(9.5) to get

$$\frac{d \ln g(L)}{d \ln L} = \frac{L}{g} \frac{dg}{dL} = \frac{L}{g} \frac{dg(nL)}{dL} \bigg|_{n=1} = \frac{1}{g} \frac{dg(nL)}{dn} \bigg|_{n=1} = \frac{1}{g} \frac{df(n, g)}{dn} \bigg|_{n=1} \equiv \beta(g). \quad (9.7)$$

The physical significance of the scaling function, β , is as follows: If we start out with a block of size L , with a value of the conductance $g(L)$ for which $\beta(g)$ is positive, then the conductance according to eq.(9.6) will increase upon enlarging the system, and vice versa for $\beta(g)$ negative. The β -function thus specifies the

²Thouless [37].

²We are thus assuming that it is meaningful to describe the current density through a local relation between current and field, $\mathbf{j} = \sigma \mathbf{E}$. Clearly the size of the system must be larger than the mean free path, $L > l$.

transport properties at that degree of disorder for a system in the thermodynamic, infinite volume, limit.

In the limit of weak disorder, large conductance $g \gg 1$, we expect metallic conduction to prevail. The conductance is thus described by classical transport theory as in relation eq.(9.3), and we obtain the limiting behavior for the scaling function

$$\beta(g) = d - 2, \quad g \gg 1 \quad (9.8)$$

the scaling function having an asymptotic limit depending only on the dimensionality of the system.

In the limit of strong disorder, small conductance $g \ll 1$, we expect with Anderson [35] that localization prevails, so that the conductance assumes the form $g(L) \propto e^{-L/\xi}$, where ξ is called the localization length, the length scale beyond which the resistance grows exponentially with length.³ In the low conductance, so-called strong localization, regime we thus obtain for the scaling function, c being a constant,

$$\beta(g) = \ln g + c, \quad g \ll 1 \quad (9.9)$$

a logarithmic dependence in any dimension.

Since there is no intrinsic length scale to tell us otherwise, it is physically reasonable in this consideration to draw the scaling function as a monotonic non-singular function connecting the two asymptotes. We therefore obtain the behavior of the scaling function depicted in figure 9.1. This is precisely the picture expected in three and one dimensions. In three dimensions the unstable fix-point signals the metal-insulator transition predicted by Anderson. The transition occurs at a critical value of the disorder where the scaling function vanishes, $\beta(g_c) = 0$. If we start with a sample with conductance larger than the critical value, $g > g_c$, then upon increasing the size of the sample the conductance increases since the scaling function is positive. In the thermodynamic limit, the system becomes a metal with conductivity σ_0 . Conversely, starting with a more disordered sample with conductance less than the critical value, $g < g_c$, upon increasing the size of the system, the conductance will flow to the insulating regime, since the scaling function is negative. In the thermodynamic limit the system will be an insulator with zero conductance. This is the localized state. In one dimension it can be shown that all states are exponentially localized for arbitrarily small amount of disorder [39], and the metallic state is absent, in accordance with the scaling function being negative. An astonishing prediction follows from the scaling theory in the two-dimensional case where the one-parameter scaling function is also negative. There is no true metallic state in two dimensions!⁴

³This expectation we demonstrate to hold true in section 9.3.5. At this point we just argue that if the envelope function for a typical electronic wave function is exponentially localized, the conductance will have the stated length dependence, where ξ is the localization length of a typical wave function in the random potential, as it is proportional to the probability for the electron to be at the edge of the sample.

⁴In this day and age, low-dimensional electron systems are routinely manufactured. For example, a two-dimensional electron gas can be created in the inversion layer of an MBE grown GaAs-AlGaAs heterostructure. Two-dimensional localization effects provide a useful tool for

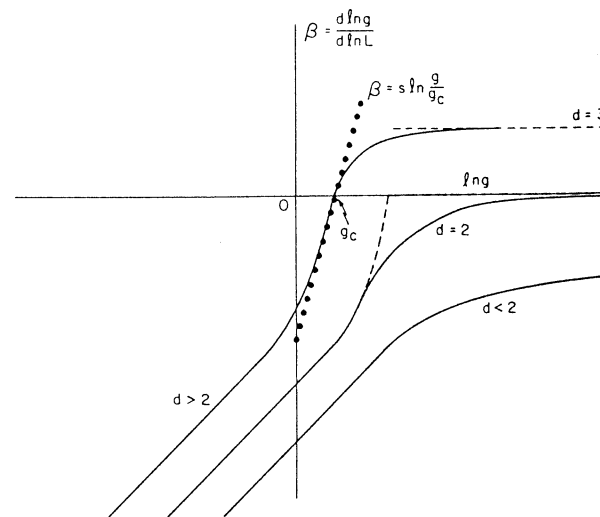


Figure 9.1 The scaling function as function of $\ln g$ (from E. Abrahams, P. W. Anderson, D. C. Licciardello, and T. V. Ramakrishnan, Phys. Rev. Lett. **42**, 673 (1979)).

The prediction of the scaling theory of the absence of a true metallic state in two dimensions was at variance with the previously conjectured theory of *minimal metallic conductivity*. The classical conductivity obtained from the Boltzmann theory has the form, in two and three dimensions ($d = 2, 3$),⁵

$$\sigma_0 = \frac{e^2}{h} \frac{k_F l}{d\pi^{d-1}} k_F^{d-2}. \quad (9.10)$$

According to Mott, the conductivity in three (and two) spatial dimensions should decrease as the disorder increases, until the mean free path becomes of the order of the Fermi wavelength of the electron, $l \sim \lambda_F$. The minimum metallic conductivity should thus occur for the amount of disorder for which $k_F l \sim 2\pi$, and in two dimensions have the universal value e^2/h . Upon further increasing the disorder, the conductivity should discontinuously drop to zero.⁶ This is in contrast to the scaling theory, which predicts the conductivity to be a continuous function of disorder. The metal-insulator transition thus resembles a second-order phase transition, in contrast to Mott's first-order conjecture (corresponding to a scaling function represented by the dashed line in the above figure).⁷

probing material characteristics, as we discuss in chapter 11.

⁵In one dimension, the Boltzmann conductivity is $\sigma_0 = 2e^2/\pi h$. However, the conclusion to be drawn from the scaling theory is that even the slightest amount of disorder invalidates the Boltzmann theory in one and two dimensions.

⁶In three dimensions in the thermodynamic limit the *conductance* drops to zero at the critical value according to the scaling theory.

⁷The impressive experimental support for the existence of a minimal metallic conductivity

The phenomenological scaling theory offers a comprehensive picture of the conductance of disordered systems, and predicts that all states in two dimensions are localized irrespective of the amount of disorder. To gain confidence in this surprising result, one should check the first correction to the metallic limit. We therefore calculate the first quantum correction to the scaling function and verify that it is indeed negative.

9.2 Coherent Backscattering

In diagrammatic terms, the quantum corrections to the classical conductivity are described by conductivity diagrams where impurity lines connecting the retarded and advanced lines cross. Such diagrams are smaller, determined by the quantum parameter $\hbar/p_F l$, than the classical contribution. The subclass of diagrams, where the impurity lines cross a maximal number of times, is of special importance since their sum exhibits singular behavior (as we already noted in section 8.10). Such a type of diagram is illustrated below:

The maximally crossed diagrams describe the first quantum correction to the classical conductivity, the weak-localization effect, a subject we discuss in full detail in chapter 11.

In the frequency and wave vector region of interest each insertion in a maximally crossed diagram is of order 1, just as in the case of the ladder diagrams. Diagrams with maximally crossing impurity lines are therefore all of the same order of magnitude and must accordingly all be summed ($\hbar Q \equiv \mathbf{p} + \mathbf{p}'$);

From the maximally crossed diagrams, we obtain analytically, by applying the Feynman rules, the correction to the conductivity of a degenerate Fermi gas,

in two dimensions is now believed to either reflect the cautiousness one must exercise when attempting to extrapolate measurements at finite temperature to zero temperature, or invoke a crucial importance of electron-electron interaction in dirty metals even at very low temperatures.

$$\hbar\omega, kT \ll \epsilon_F,^8$$

$$\delta\sigma_{\alpha,\beta}(\mathbf{q}, \omega) = \left(\frac{e}{m}\right)^2 \frac{\hbar}{\pi} \int \frac{d\mathbf{p}}{(2\pi\hbar)^d} \int \frac{d\mathbf{p}'}{(2\pi\hbar)^d} p_\alpha p'_\beta \tilde{C}_{\mathbf{p},\mathbf{p}'}(\epsilon_F, \mathbf{q}, \omega) G^R(\mathbf{p}_+, \epsilon_F + \hbar\omega) G^R(\mathbf{p}'_+, \epsilon_F + \hbar\omega) G^A(\mathbf{p}'_-, \epsilon_F) G^A(\mathbf{p}_-, \epsilon_F). \quad (9.13)$$

To describe the sum of the maximally crossed diagrams, we have introduced the so-called Cooperon \tilde{C} ,⁹ corresponding to the diagrams ($\epsilon_F^\pm \equiv \epsilon_F \pm \hbar\omega$)

$$\begin{aligned} \tilde{C}_{\mathbf{p},\mathbf{p}'}(\epsilon_F, \mathbf{q}, \omega) &\equiv \text{Diagram 1} \\ &\equiv \text{Diagram 2} + \text{Diagram 3} + \dots \\ &= \text{Diagram 4} \\ &+ \text{Diagram 5} + \dots \quad (9.14) \end{aligned}$$

The diagrams are Feynman diagrams representing the Cooperon. Diagram 1 is a bubble with two vertices, each having two external lines. Diagram 2 is a more complex diagram with multiple internal lines and vertices. Diagram 3 is another complex diagram. Diagram 4 is a diagram with two vertices and two internal lines. Diagram 5 is a diagram with two vertices and two internal lines, similar to Diagram 4 but with different internal line labels.

⁸In fact we shall in this section assume zero temperature as we shall neglect any influence on the maximally crossed diagrams from inelastic scattering. Interaction effects will be the main topic of section 11.3.

⁹The nickname refers to the singularity in its momentum dependence being for zero total momentum, as is the case for the Cooper pairing correlations resulting in the superconductivity instability.

In the last equality we have twisted the A -line around in each of the diagrams, and by doing so, we of course do not change the numbers being multiplied together.

Let us consider the case where the random potential is delta-correlated¹⁰

$$\langle V(\mathbf{x})V(\mathbf{x}') \rangle = u^2 \delta(\mathbf{x} - \mathbf{x}'). \quad (9.15)$$

Since the impurity correlator in the momentum representation then is a constant, u^2 , all internal momentum integrations become independent. As a consequence, the dependence of the Cooperon on the external momenta will only be in the combination $\mathbf{p} + \mathbf{p}'$, for which we introduce the notation $\hbar\mathbf{Q} \equiv \mathbf{p} + \mathbf{p}'$, as well as $\tilde{C}_\omega(\mathbf{p} + \mathbf{p}') \equiv \tilde{C}_{\mathbf{p},\mathbf{p}'}(\epsilon_F, \mathbf{0}, \omega) \equiv \tilde{C}_\omega(\mathbf{Q})$, and we have

$$\begin{aligned} \tilde{C}_\omega(\mathbf{Q}) &= \text{Diagram 6} + \text{Diagram 7} + \dots \\ &= \text{Diagram 8} \left(1 + \text{Diagram 9} + \dots \right) \\ &+ \text{Diagram 10} + \dots \\ &\equiv \text{Diagram 11} \cdot \text{Diagram 12} \quad (9.16) \end{aligned}$$

The diagrams are Feynman diagrams representing the Cooperon. Diagram 6 is a diagram with two vertices and two internal lines. Diagram 7 is a diagram with two vertices and two internal lines. Diagram 8 is a diagram with two vertices and two internal lines. Diagram 9 is a diagram with two vertices and two internal lines. Diagram 10 is a diagram with two vertices and two internal lines. Diagram 11 is a diagram with two vertices and two internal lines. Diagram 12 is a diagram with two vertices and two internal lines.

¹⁰As we already noted in section 8.5, the case of a short-range potential goes through as usual, the only change being the appearance of the transport time instead of the momentum relaxation time. For a discussion of the effects of anisotropy we refer to [40].

For convenience we have extracted a factor from the maximally crossed diagrams which we shortly demonstrate, eq.(9.23), is simply the constant u^2 in the relevant parameter regime. We shall therefore also refer to C as the Cooperon. Diagrammatically we obtain according to eq.(9.16)

$$\boxed{C} = 1 + \begin{array}{c} \text{R} \\ \text{p}''_+ \\ \text{A} \\ \hline \text{hQ} - \text{p}''_+ \end{array} \boxed{C} \quad (9.17)$$

Analytically the Cooperon satisfies the equation

$$C_\omega(\mathbf{Q}) = 1 + u^2 \int \frac{d\mathbf{p}''}{(2\pi\hbar)^d} G^R(\mathbf{p}''_+, \epsilon_F + \hbar\omega) G^A(\mathbf{p}''_+ - \hbar\mathbf{Q}, \epsilon_F) C_\omega(\mathbf{Q}) \quad (9.18)$$

It is obvious that a change in the wave vector of the external field can be compensated by a shift in the momentum integration variable, leaving the Cooperon independent of any spatial inhomogeneity in the electric field which is smooth on the atomic scale.

The Cooperon equation is a simple geometric series which we immediately can sum¹¹

$$\begin{aligned} C_\omega(\mathbf{Q}) &= (1 + \zeta(\mathbf{Q}, \omega) + \zeta^2(\mathbf{Q}, \omega) + \zeta^3(\mathbf{Q}, \omega) + \dots) \\ &= 1 + \zeta(\mathbf{Q}, \omega) C_\omega(\mathbf{Q}) \\ &= \frac{1}{1 - \zeta(\mathbf{Q}, \omega)} \end{aligned} \quad (9.19)$$

Diagrammatically we can express the result

$$C_\omega(\mathbf{Q}) = \frac{1}{1 - \begin{array}{c} \text{R} \\ \text{p}''_+ \\ \text{A} \\ \hline \text{hQ} - \text{p}''_+ \end{array}} \quad (9.20)$$

We have previously calculated the insertion $\zeta(\mathbf{Q}, \omega)$, eq.(8.69), and for the region of interest, $\omega\tau, Ql \ll 1$, we have

$$\zeta(\mathbf{Q}, \omega) = 1 + i\omega\tau - D_0\tau Q^2 \quad (9.21)$$

¹¹This result we already derived in section 8.10, where we established the relation between the Diffuson and its twisted diagrams in the case of time-reversal invariance.

and for the Cooperon

$$C_\omega(\mathbf{Q}) = \frac{1}{-i\omega + D_0Q^2} \quad (9.22)$$

The Cooperon exhibits singular infrared behavior.

In the singular region the prefactor in eq.(9.16) equals the constant u^2 as

$$\begin{array}{c} \text{R} \\ \text{p}''_+ \\ \text{A} \\ \hline \text{hQ} - \text{p}''_+ \end{array} = u^2 \zeta(\mathbf{Q}, \omega) \simeq u^2 \quad (9.23)$$

i.e., in the region of interest we thus have $\tilde{C} = u^2 C$. As far as regards the singular behavior we could equally well have defined the Cooperon by the set of diagrams

$$\begin{aligned} \tilde{C}_\omega(\mathbf{Q}) &= \begin{array}{c} \text{---} \\ \text{---} \\ \text{---} \end{array} + \begin{array}{c} \text{R} \\ \text{p}_+ \leftarrow \text{p}'_+ \\ \text{A} \\ \text{p}'_- \leftarrow \text{p}_- \\ \text{hQ} - \text{p}_+ \end{array} \\ &+ \begin{array}{c} \text{R} \quad \text{R} \\ \text{p}_+ \leftarrow \text{p}'_+ \quad \text{p}'_+ \leftarrow \text{p}_+ \\ \text{A} \quad \text{A} \\ \text{p}'_- \leftarrow \text{p}_- \quad \text{p}_- \leftarrow \text{p}'_- \\ \text{hQ} - \text{p}_+ \quad \text{hQ} - \text{p}_+ \end{array} + \dots \end{aligned} \quad (9.24)$$

as adding a constant to a singular function does not change the singular behavior.

Changing in the conductivity expression, eq.(9.13), one of the integration variables, $\mathbf{p}' = -\mathbf{p} + \hbar\mathbf{Q}$, we get for the contribution of the maximally crossed diagrams

$$\begin{aligned} \delta\sigma_{\alpha\beta}(\mathbf{q}, \omega) &= \left(\frac{e}{m}\right)^2 \frac{\hbar}{\pi} \int \frac{d\mathbf{p}}{(2\pi\hbar)^d} \int \frac{d\mathbf{Q}}{(2\pi)^d} p_\alpha(-\mathbf{p}_\beta + \hbar\mathbf{Q}_\beta) \frac{u^2/\tau}{-i\omega + D_0Q^2} \\ &G_{\epsilon_F}^R(\mathbf{p}_+) G_{\epsilon_F}^R(-\mathbf{p}_+ + \hbar\mathbf{Q}) G_{\epsilon_F}^A(-\mathbf{p}_- + \hbar\mathbf{Q}) G_{\epsilon_F}^A(\mathbf{p}_-) \end{aligned} \quad (9.25)$$

where the prime on the \mathbf{Q} -integration signifies that we only need to integrate over the region $Ql < 1$ from which the large contribution is obtained. Everywhere

except in the Cooperon we can therefore neglect \mathbf{Q} as $|\mathbf{p} - \hbar\mathbf{Q}| \sim p \sim p_F$. Assuming a smoothly varying external field on the atomic scale, $q \ll k_F$,¹² we can perform the momentum integration, and obtain to leading order in $\hbar/p_F l$

$$\int \frac{d\mathbf{p}}{(2\pi\hbar)^d} p_\alpha p_\beta G_{\epsilon_F}^R(\mathbf{p}_+) G_{\epsilon_F}^R(-\mathbf{p}_+) G_{\epsilon_F}^A(-\mathbf{p}_-) G_{\epsilon_F}^A(\mathbf{p}_-) = \frac{4\pi\tau^3 N_d(\epsilon_F) p_F^2}{\hbar^3 d} \delta_{\alpha\beta} \quad (9.26)$$

where we have also safely neglected the ω dependence in the propagators as for the region giving the large contribution, we have $\omega < 1/\tau \ll \epsilon_F/\hbar$.

At zero frequency we have for the first quantum correction to the conductivity of an electron gas

$$\delta\sigma(L) = -\frac{2e^2 D_0}{\pi\hbar} \int \frac{d\mathbf{Q}}{(2\pi)^d} \frac{1}{D_0 Q^2}. \quad (9.27)$$

In the one- and two-dimensional case the integral diverges for small Q , and we need to assess the lower cut-off.¹³ In order to understand the lower cut-off we note that the maximally crossed diagrams lend themselves to a simple physical interpretation. The R -line in the Cooperon describes the amplitude for the scattering sequence of an electron (all momenta being near the Fermi surface as the contribution is otherwise small)

$$\mathbf{p}' \rightarrow \mathbf{p}_1 \rightarrow \dots \rightarrow \mathbf{p}_N \rightarrow \mathbf{p} \simeq -\mathbf{p}' \quad (9.28)$$

whereas the A -line describes the complex conjugate amplitude for the opposite, i.e., time-reversed, scattering sequence

$$\mathbf{p}' \rightarrow -\mathbf{p}_N \rightarrow \dots \rightarrow -\mathbf{p}_1 \rightarrow \mathbf{p} \simeq -\mathbf{p}' \quad (9.29)$$

i.e., the Cooperon describes a quantum interference process: the quantum interference between time-reversed scattering sequences. The physical process responsible for the quantum correction is thus coherent backscattering.¹⁴ The random potential acts as sets of mirrors such that an electron in momentum state \mathbf{p} ends up backscattered into momentum state $-\mathbf{p}$. The quantum correction to the conductivity is thus negative as the conductivity is a measure of the initial and final correlation of the velocities as reflected in the factor $\mathbf{p} \cdot \mathbf{p}'$ in the conductivity expression.

¹²In a conductor a spatially varying electric field will due to the mobile charges be screened (as we discuss further in section 10.5). In a metal, say, an applied electric field is smoothly varying on the atomic scale, $q \ll k_F$, and we can set q equal to zero as it appears in combination with large momenta, $p, p' \sim p_F$.

¹³Langer and Neal [41] were the first to study the maximally crossed diagrams, and noted that they give a divergent result at zero temperature. However, in their analysis they did not assess the lower cut-off correctly.

¹⁴The coherent backscattering effect was considered for light waves already in 1968 [42]. It is amusing that a quantitative handling of the phenomena had to await the study of the analogous effect in solid-state physics, and the diagrammatic treatment of electronic transport in metals a decade later.

The quantum interference process described by the above scattering sequences corresponds in real space to the quantum interference between the two alternatives for a particle to traverse a closed loop in opposite (time-reversed) directions.¹⁵

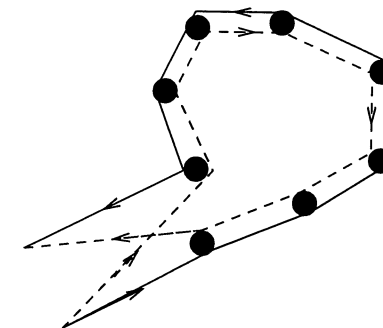


Figure 9.2 Coherent backscattering process.

We are considering the phenomenon of conductivity, where currents through connecting leads are taken in and out of a sample, say, at opposing faces of a hypercube. The maximal size of a loop allowed to contribute to the coherent backscattering process is thus the linear size of the system, as we assume that an electron reaching the end of the sample is irreversibly lost to the environment (leads and battery). For a system of linear size L we then have for the quantum correction to the conductivity

$$\delta\sigma(L) = -\frac{2e^2 D_0}{\pi\hbar} \int_{1/L}^{1/l} \frac{d\mathbf{Q}}{(2\pi)^d} \frac{1}{D_0 Q^2}. \quad (9.30)$$

Performing the integral in the two-dimensional case gives for the first quantum correction to the dimensionless conductance¹⁶

$$\delta g(L) = -\frac{1}{\pi^2} \ln \frac{L}{l}. \quad (9.31)$$

We note that the first quantum correction to the conductivity indeed is negative, describing the precursor effect of localization. For the asymptotic scaling function we then obtain

$$\beta(g) = -\frac{1}{\pi^2 g}, \quad g \gg 1 \quad (9.32)$$

¹⁵This all important observation of the physical origin of the quantum correction to the conductivity (originally expressed in reference [43]) we shall take advantage of in chapter 11, where the real space treatment of weak localization is done in detail.

¹⁶The precise magnitudes of the cutoffs are irrelevant for the scaling function in the two-dimensional case, as a change can only produce the logarithm of a constant in the dimensionless conductance.

and the first quantum correction to the scaling function is thus seen to be negative in concordance with the scaling picture.

Exercise 9.1 Show that in dimensions one and three we get for the first quantum correction to the dimensionless conductance

$$\delta g(L) = \begin{cases} -\frac{1}{\pi}(1 - \frac{1}{L}) & d = 1 \\ -\frac{1}{\pi^3}(\frac{L}{l} - 1) & d = 3 \end{cases} \quad (9.33)$$

and thereby for the scaling function to lowest order in $1/g$

$$\beta(g) = (d-2) - \frac{a}{g} \quad (9.34)$$

where

$$a = \begin{cases} \frac{1}{2} & d = 1 \\ \frac{1}{\pi^3} & d = 3 \end{cases} \quad (9.35)$$

We introduce the length scale describing localization, the localization length, as follows: for a sample much larger than the localization length, $L \gg \xi$, the sample is in the localized regime and we have $g(L) \simeq 0$. To estimate the localization length, we equate it to the length for which $g(\xi) \simeq g_0$, i.e., the length scale where the scale dependent part of the conductance is comparable to the Boltzmann conductance. The lowest-order perturbative estimate based on eq.(9.31) and eq.(9.33) gives in two and one dimensions the localization lengths $\xi^{(2)} \simeq l \exp \pi k_F l / 2$ and $\xi^{(1)} \simeq l$, respectively.

The one-parameter scaling hypothesis has been shown to be valid for the average conductance in the above considered model [36]. Whether the one-parameter scaling picture for the disorder model studied is true for higher-order cumulants of the conductance, $\langle g^n \rangle$, is a difficult question which seems to have been answered in the negative in reference [44]. However, a different question is whether deviations from one-parameter scaling are observable, in the sense that a sample has to be so close to the metal-insulator transition that real systems cannot be made homogeneous enough. Furthermore, electron-electron interaction can play a profound role in real materials invalidating the model studied, and leaving room for a metal-insulator transition in low-dimensional systems [45].

We can also calculate the zero-temperature frequency dependence of the first quantum correction to the conductivity for a sample of large size, $L \gg \sqrt{D_0/\omega} \equiv L_\omega$. From eq.(9.25) we have

$$\delta \sigma_{\alpha\beta}(\omega) = \delta \sigma(\omega) \delta_{\alpha\beta} \quad (9.36)$$

where

$$\delta \sigma(\omega) = -\frac{2e^2 D_0}{\hbar \pi} \int_0^{1/l} \frac{d\mathbf{Q}}{(2\pi)^d} \frac{1}{-i\omega + D_0 Q^2} \quad (9.37)$$

Calculating the integral, we get for the frequency dependence of the quantum correction to the conductivity in, say, two dimensions [46]

$$\frac{\delta \sigma(\omega)}{\sigma_0} = -\frac{1}{\pi k_F l} \ln \frac{1}{\omega \tau} \quad (9.38)$$

We note that for the perturbation theory to remain valid the frequency can not be too small, $\omega \tau \simeq 1$.

The quantum correction to the conductivity in two dimensions is seen to be universal

$$\delta \sigma(\omega) = -\frac{1}{2\pi^2} \frac{e^2}{\hbar} \ln \frac{1}{\omega \tau} \quad (9.39)$$

Let us calculate the first quantum correction to the current density response to a spatially homogeneous electric pulse, recall eq.(8.81),

$$\delta \mathbf{j}(t) = \delta \sigma(t) \mathbf{E}_0 \quad (9.40)$$

where

$$\delta \sigma(t) = -\frac{2e^2 D_0}{\hbar \pi} \int_{-\infty}^{\infty} \frac{d\omega}{2\pi} e^{-i\omega t} \int_{1/L}^{1/l} \frac{d\mathbf{Q}}{(2\pi)^d} \frac{1}{-i\omega + D_0 Q^2} = -\frac{2e^2 D_0}{\hbar \pi} \int_{1/L}^{1/l} \frac{d\mathbf{Q}}{(2\pi)^d} e^{-iD_0 Q^2 t} \quad (9.41)$$

which in the two-dimensional case becomes

$$\delta \sigma(t) = \frac{e^2}{2\pi^2 \hbar t} \left(e^{-\frac{t}{2\tau}} - e^{-\frac{D_0 t}{L^2}} \right) \quad (9.42)$$

After the short time τ the classical contribution, eq.(8.84), and the above quantum contribution in the direction of the force on the electron dies out, and an *echo* in the current due to coherent backscattering occurs

$$\mathbf{j}(t) = -\frac{e^2}{2\pi^2 \hbar t} e^{-t/\tau_D} \mathbf{E}_0 \quad (9.43)$$

on the large time scale $\tau_D \equiv L^2/D_0$, the time it takes an electron to diffuse across the sample (for even larger times $t \gg \tau_D$ quantum corrections beyond the first dominates the current).

Exercise 9.2 Show that in dimensions 1 and 3 we get for the frequency dependence of the first quantum correction to the conductivity

$$\frac{\delta\sigma(\omega)}{\sigma_0} = \begin{cases} \frac{-\pi}{\sqrt{2}} \frac{1}{\sqrt{\omega\tau}} & d = 1 \\ \frac{3\sqrt{6\omega\tau}}{2(k_F l)^2} & d = 3. \end{cases} \quad (9.44)$$

In dimension d the quantum correction to the conductivity is of relative order $1/(k_F l)^{d-1}$. In strictly one dimension the weak localization regime is thus absent; i.e., there is no regime where the first quantum correction is small compared to the Boltzmann result, we are always in the strong localization regime.

From the formulas, eq.(7.142) and eq.(9.39), we find that in a quasi-two-dimensional system, where the thickness of the film is much smaller than the length scale introduced by the frequency of the time-dependent external field, $L_\omega \equiv (D_0/\omega)^{1/2}$, the quantum correction to the conductance exhibits the singular frequency behavior

$$\delta \langle G_{\alpha\beta}(\omega) \rangle = -\frac{e^2}{2\pi^2\hbar} \delta_{\alpha\beta} \ln \frac{1}{\omega\tau}. \quad (9.45)$$

The quantum correction to the conductance is in the limit of a large two-dimensional system only finite because we consider a time-dependent external field, and the conductance increases with the frequency. This feature can be understood in terms of the coherent backscattering picture. In the presence of the time-dependent electric field the electron can at arbitrary times exchange a quantum of energy $\hbar\omega$ with the field, and the coherence between two otherwise coherent alternatives will be partially disrupted. The more ω increases, the more the coherence of the backscattering process is suppressed, and consequently the tendency to localization, as a result of which the conductivity increases.

The first quantum correction plays a role even at finite temperatures, and in chapter 11 we show that from an experimental point of view there are important quantum corrections to the Boltzmann conductivity even at weak disorder. We have realized that if we can break the time-reversal invariance for the electron dynamics, we can disrupt the coherence in the backscattering process, and suppress localization. The interaction of an electron with its environment invariably breaks the coherence, and we discuss the effects of electron-phonon and electron-electron interaction in section 11.3. A more distinct probe for influencing localization is to apply a magnetic field which we discuss in section 11.4.

We have realized that the precursor effect of localization, weak localization, is due to coherent backscattering. The constructive interference between time-reversed loops, which increases the probability for a particle to return to its starting position. The phenomenon of localization can be understood qualitatively as follows: The main amplitude of the electronic wave function incipient on the first

impurity in figure 9.2 is not scattered into the loop depicted, but continues in its forward direction. However, this part of the wave also encounters coherent backscattering along another closed loop feeding constructively back into the original loop, and thereby increasing the probability of return. This process repeats at any impurity, and the random potential acts as a mirror, making it impossible for a particle to diffuse away from its starting point. We now turn to a quantitative discussion of localization.

9.3 Self-consistent Theory of Localization

In the previous section we indeed demonstrated that the first quantum correction to the conductance is negative in concordance with the prediction of the scaling theory of localization. We shall now go beyond first-order perturbation theory in the quantum parameter λ_F/l , and construct the self-consistent theory of localization following reference [34]. The self-consistent theory¹⁷ provides a good approximate description of Anderson localization, as comparison with numerical results testify, except possibly very close to the metal-insulator transition in three dimensions.¹⁸ To probe the motion of the electrons we shall consider the density response, which according to eq.(8.169) is specified by the diffusivity. In order to establish the self-consistent theory of localization we shall utilize the diagrammatic structure of the skeleton perturbation expansion of the four-point function describing the motion of a particle in a random potential. We assume for simplicity the isotropic scattering model where $\tau_{tr} = \tau$.

9.3.1 Weak-Localization Regime

In the previous section it was shown that the first quantum correction to the conductivity is governed by the infra-red (small ω) behavior of the Cooperon. Let us therefore first investigate the contribution from the Cooperon to the diffusivity; i.e., we approximate the irreducible vertex U in eq.(8.159) by the Cooperon $\tilde{C}_\omega(\mathbf{p} + \mathbf{p}')$, and obtain in this approximation for the diffusivity (for $q \ll k_F$ we can set \mathbf{q} equal to zero)

$$\frac{D_0}{\tilde{D}_C(\omega)} = 1 + \frac{d\tau}{\pi\hbar mn V^2} \sum'_{\mathbf{p}, \mathbf{p}'} (\mathbf{p} \cdot \hat{\mathbf{q}}) \Delta G_{\mathbf{p}} \left[\frac{u^2/\tau}{-i\omega + D_0(\mathbf{p} + \mathbf{p}')^2\hbar^{-2}} \right] (\mathbf{p}' \cdot \hat{\mathbf{q}}) \Delta G_{\mathbf{p}'} \quad (9.46)$$

¹⁷As all self-consistent theories, such as also the one we employ in the next chapter to describe the electron-electron interaction in a metal, it is uncontrolled, in the sense that no small parameter estimates the accuracy of the theory. However, we do not have any general tool to calculate properties of strongly interacting many-body systems (except in one-dimensional systems, where it is possible to obtain exact results).

¹⁸In the field theoretic formulation of the localization problem, the self-consistent theory is known to be equivalent to in the effective action to keep all vacuum diagrams up to two-particle irreducible level; see reference [47].

where the prime indicates that the summation is restricted to the singular region $|\mathbf{p} + \mathbf{p}'| < \hbar/l$. Changing momentum variable to the total momentum, $\hbar\mathbf{Q} \equiv \mathbf{p} + \mathbf{p}'$, we obtain

$$\frac{D_0}{\tilde{D}_C(\omega)} = 1 + \frac{d\tau}{\pi\hbar mnV^2} \sum'_{\mathbf{p}, \mathbf{Q}} (\mathbf{p} \cdot \hat{\mathbf{q}}) \Delta G_{\mathbf{p}} \left[\frac{u^2/\tau}{-i\omega + D_0 Q^2} \right] (\hbar\mathbf{Q} - \mathbf{p}) \cdot \hat{\mathbf{q}} \Delta G_{\hbar\mathbf{Q}-\mathbf{p}}. \quad (9.47)$$

The singular behavior of the Cooperon is in the small Q -limit, $Ql \ll 1$, so that Q can be set to zero in the spectral function which is peaked at k_F , leading to the simplification of the expression eq.(9.47)

$$\frac{D_0}{\tilde{D}_C(\omega)} = 1 - \frac{d\tau}{\pi\hbar mnV^2} \sum'_{\mathbf{p}, \mathbf{Q}} (\mathbf{p} \cdot \hat{\mathbf{q}})^2 (\Delta G_{\mathbf{p}})^2 \left[\frac{u^2/\tau}{-i\omega + D_0 Q^2} \right]. \quad (9.48)$$

The momentum integral is readily evaluated, and the diffusivity is to lowest order in the quantum parameter given by

$$\begin{aligned} \frac{D_0}{\tilde{D}_C(\omega)} &= 1 + \frac{1}{\pi\hbar N_0 V} \sum'_{\mathbf{Q}} \frac{1}{-i\omega + D_0 Q^2} \\ &= 1 + \frac{1}{k_F l} \frac{d}{\pi} k_F^{2-d} \int_0^{1/l} dQ \frac{Q^{d-1}}{-i\omega/D_0 + Q^2}. \end{aligned} \quad (9.49)$$

In less than two dimensions, $d \leq 2$, the first quantum correction is seen to diverge

$$\frac{D_0}{\tilde{D}_C(\omega)} - 1 = \left(\frac{\hbar}{\pi p_F l} \right)^{d-1} \begin{cases} \frac{\pi}{\sqrt{2}} \frac{1}{\sqrt{\omega\tau}} & d = 1 \\ \ln \frac{1}{\omega\tau} & d = 2. \end{cases} \quad (9.50)$$

In order for perturbation theory to be valid, the zero frequency limit can not be taken. If, on the other hand, ω is not too small, the second term in the expression eq.(9.49) is much less than one, and from the Einstein relation, eq.(8.170), the weak-localization expression for the conductivity is recovered

$$\frac{\delta\sigma(\omega)}{\sigma_0} = -\frac{\hbar}{p_F l} \frac{d}{\pi} k_F^{2-d} \int_0^{1/l} dQ \frac{Q^{d-1}}{-i\omega/D_0 + Q^2}. \quad (9.51)$$

However, the zero frequency limit is precisely the one of interest as localization is signaled by the infrared divergence of the inverse diffusivity, $K(\omega)$. Based on the perturbative result, eq.(9.49), a natural guess for a self-consistent equation for the diffusivity is obtained by substituting on the right-hand side of eq.(9.49) the diffusivity instead of the diffusion constant

$$\frac{D_0}{\tilde{D}(\omega)} = 1 + \frac{1}{\pi\hbar N_0 V} \sum'_{\mathbf{Q}} \left[\frac{1}{-i\omega + \tilde{D}(\omega) Q^2} \right]. \quad (9.52)$$

Obtaining this conjectured self-consistent equation can be based on a diagrammatic classification. In order to obtain the result, the key point to notice is that a

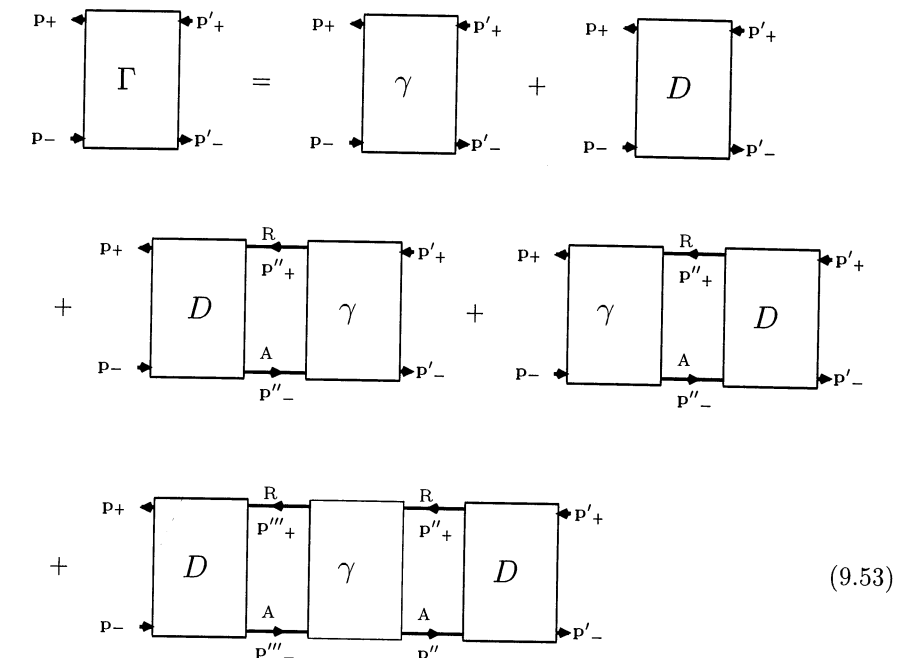
quantity where exactly the desired denominator appears is known, viz. the four-point function $\Phi(\mathbf{q}, \omega)$ of eq.(8.167). If the irreducible four-point function U can be related to Φ , a self-consistent equation for \tilde{D} is thus according to eq.(8.159) obtained.

9.3.2 Self-consistent Equation

We now demonstrate that the conjectured self-consistent equation for the diffusivity, eq.(9.52), can be justified diagrammatically by taking into account the most singular contribution to the irreducible vertex function $U_{\mathbf{p}, \mathbf{p}'}$.

A four point vertex diagram can be classified according to whether it is *immediately left or right two-line reducible*, i.e., has an impurity correlator (or t -matrix) line connecting the particle lines at the utmost right or left of the diagram. We define the auxiliary four-point vertex consisting of all *immediately left and right two-line irreducible* diagrams, i.e., the sum of all the diagrams which have no impurity line connecting the R and A line at the very right or left of the diagram. This vertex function is denoted $\gamma_{\mathbf{p}, \mathbf{p}'}(\mathbf{q}, \omega)$.

The four-point vertex consists of the *immediately left and right irreducible* diagrams γ , the Diffuson D , the *immediately left reducible* diagrams, and the *immediately right reducible* diagrams, and finally the both *immediately left and right reducible* diagrams



$$\begin{aligned} \Gamma &= \gamma + D \\ &+ \left(D \begin{matrix} \text{R} \\ \text{p}''_+ \\ \text{A} \\ \text{p}''_- \end{matrix} \gamma \right) + \left(\gamma \begin{matrix} \text{R} \\ \text{p}''_+ \\ \text{A} \\ \text{p}''_- \end{matrix} D \right) \\ &+ \left(D \begin{matrix} \text{R} \\ \text{p}'''_+ \\ \text{A} \\ \text{p}'''_- \end{matrix} \gamma \begin{matrix} \text{R} \\ \text{p}''_+ \\ \text{A} \\ \text{p}''_- \end{matrix} D \right) + \left(D \begin{matrix} \text{R} \\ \text{p}''_+ \\ \text{A} \\ \text{p}''_- \end{matrix} \gamma \begin{matrix} \text{R} \\ \text{p}'''_+ \\ \text{A} \\ \text{p}'''_- \end{matrix} D \right) + \dots \end{aligned} \quad (9.53)$$

corresponding to the equation (the energy variables, $E + \hbar\omega$ on the upper retarded line and E on the lower, advanced, line, are suppressed, and in view of eq.(8.30) fixed at the Fermi energy, $E \simeq \epsilon_F$)

$$\begin{aligned} \Gamma_{\mathbf{p},\mathbf{p}'}(\mathbf{q},\omega) &= \gamma_{\mathbf{p},\mathbf{p}'}(\mathbf{q},\omega) + D(\mathbf{q},\omega) + D(\mathbf{q},\omega) \sum_{\mathbf{p}''} R_{\mathbf{p}''}(\mathbf{q},\omega) \gamma_{\mathbf{p}'',\mathbf{p}'}(\mathbf{q},\omega) \\ &+ D(\mathbf{q},\omega) \sum_{\mathbf{p}''} \gamma_{\mathbf{p},\mathbf{p}''}(\mathbf{q},\omega) R_{\mathbf{p}''}(\mathbf{q},\omega) \\ &+ (D(\mathbf{q},\omega))^2 \sum_{\mathbf{p}'',\mathbf{p}'''} R_{\mathbf{p}'''}(\mathbf{q},\omega) \gamma_{\mathbf{p}'',\mathbf{p}'''}(\mathbf{q},\omega) R_{\mathbf{p}''}(\mathbf{q},\omega). \end{aligned} \quad (9.54)$$

The notation $R_{\mathbf{p}}(\mathbf{q},\omega) \equiv G_{\mathbf{p}+}^R G_{\mathbf{p}-}^A$ and $D(\mathbf{q},\omega) \equiv D_{\mathbf{p},\mathbf{p}'}(\mathbf{q},\omega)$ has been introduced. Furthermore, we have used the fact that since $E \simeq \epsilon_F$, $D_{\mathbf{p},\mathbf{p}'}(\mathbf{q},\omega)$ is slowly varying compared to the peaked function $R_{\mathbf{p}'}(\mathbf{q},\omega)$ in the variable \mathbf{p}' , and has been taken outside the summation. According to eq.(8.13) the function $\Phi(\mathbf{q},\omega)$ is related to the four-point vertex by

$$\begin{aligned} \Phi(\mathbf{q},\omega) &= \frac{1}{V^2} \sum_{\mathbf{p},\mathbf{p}'} \Phi_{\mathbf{p},\mathbf{p}'}(\mathbf{q},\omega) \\ &= \frac{1}{V} \sum_{\mathbf{p}} R_{\mathbf{p}}(\mathbf{q},\omega) + \frac{1}{V^2} \sum_{\mathbf{p},\mathbf{p}'} R_{\mathbf{p}}(\mathbf{q},\omega) \Gamma_{\mathbf{p},\mathbf{p}'}(\mathbf{q},\omega) R_{\mathbf{p}'}(\mathbf{q},\omega). \end{aligned} \quad (9.55)$$

For the considered case of a delta impurity correlator ($U_0 = u^2$), the four-point vertex $\Gamma_{\mathbf{p},\mathbf{p}'}(\mathbf{q},\omega)$ is independent of \mathbf{p} and \mathbf{p}' , and when the expression eq.(9.54) for Γ is inserted into eq.(9.55), we just have products over \mathbf{q},ω -dependent functions¹⁹

$$\begin{aligned} \Phi(\mathbf{q},\omega) &= R(\mathbf{q},\omega) + Z(\mathbf{q},\omega) + D(\mathbf{q},\omega) R^2(\mathbf{q},\omega) + 2D(\mathbf{q},\omega) R(\mathbf{q},\omega) Z(\mathbf{q},\omega) \\ &+ (D(\mathbf{q},\omega))^2 R^2(\mathbf{q},\omega) Z(\mathbf{q},\omega). \end{aligned} \quad (9.56)$$

The above equation can be rewritten as

$$\Phi = R(1 + DR) + Z(1 + DR)^2 \quad (9.57)$$

where we have introduced the notation

$$R = R(\mathbf{q},\omega) \equiv \frac{1}{V} \sum_{\mathbf{p}} R_{\mathbf{p}}, \quad Z = Z(\mathbf{q},\omega) \equiv \frac{1}{V^2} \sum_{\mathbf{p},\mathbf{p}'} R_{\mathbf{p}} \gamma_{\mathbf{p},\mathbf{p}'}(\mathbf{q},\omega) R_{\mathbf{p}'} \quad (9.58)$$

According to the expression for the Diffuson, eq.(8.108),

$$D \equiv D(\mathbf{q},\omega) = \frac{U_0}{1 - U_0 R} \quad (9.59)$$

¹⁹For a potential with range small compared to the mean free path, the peaked character of $R_{\mathbf{p}}$ restricts momenta to the Fermi Surface, and upon performing the angular integration the discussion is equivalent.

we have

$$1 + RD = 1 + \frac{RU_0}{1 - U_0 R} = \frac{1}{1 - U_0 R} = D U_0^{-1} \quad (9.60)$$

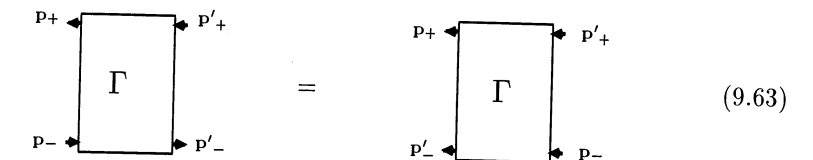
and thereby

$$1 + RD = D U_0^{-1}. \quad (9.61)$$

Using this equality we can rewrite eq.(9.57) as

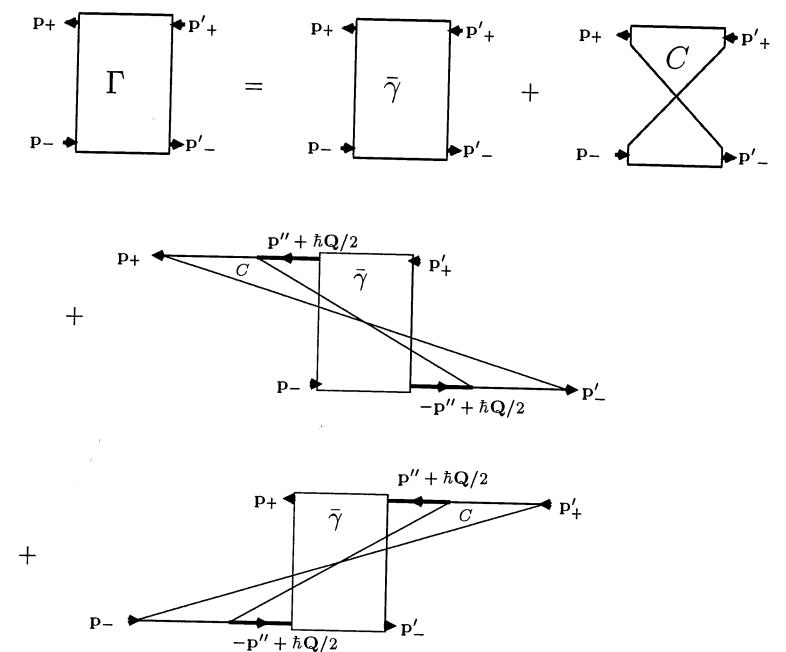
$$[D(\mathbf{q},\omega)]^2 Z(\mathbf{q},\omega) = U_0^2 \Phi(\mathbf{q},\omega) - D(\mathbf{q},\omega) + U_0. \quad (9.62)$$

Since $\Gamma_{\mathbf{p},\mathbf{p}'}(\mathbf{q},\omega)$ is the full vertex function we have according to eq.(8.172)



$$\Gamma = \gamma + \text{diagram with two crossed lines } C \quad (9.63)$$

where the particle lines on the right-hand side run parallel. The diagrammatic expansion, however, is analogous to the one in eq.(9.53) as the topological classification made no reference to the directions of the particle lines. We now twist the diagrams in this expansion on the right-hand side of eq.(9.63) and obtain



We shall now invoke time-reversal symmetry. In that case the two Cooperons in the last diagram are seen to have the same argument \mathbf{Q}, ω , where $\hbar\mathbf{Q} = \mathbf{p} + \mathbf{p}'$. The last four diagrams in eq.(9.64) are explicitly two-line irreducible, and are thus part of the irreducible vertex $U_{\mathbf{p},\mathbf{p}'}(\mathbf{q}, \omega)$. The very last diagram in eq.(9.64) contains two Cooperons with identical arguments, and are therefore more singular than the other diagrams. We therefore have for the dominant contribution to the irreducible four-point function

$$U_{\mathbf{p},\mathbf{p}'}(\mathbf{q}, \omega) \rightarrow U_{\mathbf{p},\mathbf{p}'}^{\text{domin}}(\mathbf{q}, \omega) = [C(\mathbf{p} + \mathbf{p}', \omega)]^2 Z(\mathbf{p} + \mathbf{p}', \omega) \rightarrow [C(\mathbf{p} + \mathbf{p}', \omega)]^2 Z(\mathbf{p} + \mathbf{p}', \omega) + C(\mathbf{p} + \mathbf{p}', \omega). \quad (9.65)$$

The Cooperon added in the last line, ensures that we get the correct limiting behavior in the weak-disorder limit, the aim of the self-consistent approach being to interpolate between the weak- and strong-localization regimes.

In the time reversal invariant situation we then get, using the relation eq.(9.62), for the dominant contribution to the irreducible four-point function

$$U_{\mathbf{p},\mathbf{p}'}^{\text{domin}}(\mathbf{q}, \omega) - U_0 = U_0^2 \Phi(\mathbf{p} + \mathbf{p}', \omega). \quad (9.66)$$

Inserting the dominating contribution on the right-hand side of eq.(8.159) we obtain

$$\frac{D_0}{\tilde{D}(\mathbf{q}, \omega)} = 1 + \frac{d\tau}{\pi \hbar m n V^2} \sum_{\mathbf{p}, \mathbf{p}'} (\mathbf{p} \cdot \hat{\mathbf{q}}) \Delta G_{\mathbf{p}} U_0 \Phi(\mathbf{p} + \mathbf{p}', \omega) (\mathbf{p}' \cdot \hat{\mathbf{q}}) \Delta G_{\mathbf{p}'} \quad (9.67)$$

and performing the integration over one of the momenta we have

$$\frac{D_0}{\tilde{D}(\mathbf{q}, \omega)} = 1 + \frac{1}{2(\pi N_0)^2 V} \sum_{\mathbf{Q}}' \Phi(\mathbf{Q}, \omega). \quad (9.68)$$

Upon inserting the expression eq.(8.169) yields a self-consistent equation for the diffusivity

$$\frac{D_0}{\tilde{D}(\mathbf{q}, \omega)} = 1 + \frac{\hbar k_F^{2-d}}{\pi m} \int_0^{1/l} dQ \frac{Q^{d-1}}{-i\omega + \tilde{D}(\mathbf{Q}, \omega) Q^2}. \quad (9.69)$$

The result, eq.(9.69), is independent of the small external momentum \mathbf{q} and we can set $\mathbf{q} = 0$ in $\tilde{D}(\mathbf{q}, \omega)$, and since Q is small, $Q \leq 1/l \ll k_F$, we can neglect the \mathbf{Q} -dependence in $\tilde{D}(\mathbf{Q}, \omega)$ as well, and we obtain

$$\frac{D_0}{\tilde{D}(\omega)} = 1 + \frac{\hbar k_F^{2-d}}{\pi m} \int_0^{1/l} dQ \frac{Q^{d-1}}{-i\omega + \tilde{D}(\omega) Q^2}. \quad (9.70)$$

This is precisely the self-consistent equation conjectured for the diffusivity.

We note the different roles played by the two infrared divergencies in the theory; the Diffuson, which we used to classify the diagrams of the four-point vertex, and the Cooperon, introduced by twisting the diagrams (the quantity representing the coherent backscattering process which drives the localization transition), and the crucial role of time reversal symmetry that relates the two.²⁰

Writing the equation in terms of the inverse diffusivity $K(\omega)$, eq.(8.159), we find that the solution of the self-consistent equation has at small frequencies, $\omega \ll \omega_0^2 \tau$, the form

$$K(\omega) = 1 + \frac{i\omega_0^2 \tau}{\omega} \quad (9.71)$$

where ω_0 is determined by

$$1 = \frac{\hbar k_F^{2-d}}{\pi m} \int_0^{1/l} dQ \frac{Q^{d-1}}{\omega_0^2 \tau + D_0 Q^2}. \quad (9.72)$$

In two dimensions, for example, we find from eq.(9.72) for the frequency scale where localization becomes of importance:

$$\omega_0 = \frac{1}{\sqrt{2}\tau} e^{-\frac{\pi k_F l}{2}}. \quad (9.73)$$

The discussed solution, eq.(9.71), is infrared divergent, and corresponds to the insulating phase, and the diffusivity vanishes as $\omega \rightarrow 0$ according to

$$\tilde{D}(\omega) = -i\omega \frac{D_0}{\omega_0^2 \tau}. \quad (9.74)$$

9.3.3 Localization Length

In order to get a quantitative criterion for the localization length, we can consider the spectral correlation function

$$\begin{aligned} \mathcal{A}(\mathbf{x}, \mathbf{x}', E, E + \hbar\omega) &\equiv \frac{\hbar}{\pi^2 N(E)} \langle \Im m G^R(\mathbf{x}, \mathbf{x}', E + \hbar\omega) \Im m G^R(\mathbf{x}', \mathbf{x}, E) \rangle \\ &= \frac{\hbar}{N(E)} \langle \sum_{\lambda, \lambda'} \psi_{\lambda}(\mathbf{x}) \psi_{\lambda}^*(\mathbf{x}') \psi_{\lambda'}(\mathbf{x}') \psi_{\lambda'}^*(\mathbf{x}) \delta(E + \hbar\omega - \epsilon_{\lambda'}) \delta(E - \epsilon_{\lambda}) \rangle \end{aligned} \quad (9.75)$$

where

$$N(E) = \langle \sum_{\lambda} \psi_{\lambda}(\mathbf{x}) \psi_{\lambda}^*(\mathbf{x}) \delta(E - \epsilon_{\lambda}) \rangle \quad (9.76)$$

is the impurity-averaged density of states.

²⁰It has therefore not been possible to extend the self-consistent theory to the case of broken time-reversal symmetry.

According to eq.(7.26) we have

$$\chi(\mathbf{q}, \omega) = \int_{-\infty}^{\infty} dE \int_{-\infty}^{\infty} d\omega' \frac{f_0(E + \hbar\omega') - f_0(E)}{\omega' - \omega - i0} \frac{N(E)}{\hbar} \mathcal{A}(\mathbf{q}, E, E + \hbar\omega') \quad (9.77)$$

where $\mathcal{A}(\mathbf{q}, E, E + \hbar\omega)$ is the Fourier transform of $\mathcal{A}(\mathbf{x}, \mathbf{x}', E, E + \hbar\omega)$. Since the Fourier transform is real,

$$\mathcal{A}(\mathbf{q}, E, E + \hbar\omega) = \frac{\hbar}{2\pi^2 V N(E)} \Re e \left(\Phi(E, \mathbf{q}, \omega) - \Phi^{RR}(E, \mathbf{q}, \omega) \right) \quad (9.78)$$

we have

$$\Im m \chi(\mathbf{q}, \omega) = \pi \int_{-\infty}^{\infty} dE \frac{N(E)}{\hbar} (f_0(E + \hbar\omega) - f_0(E)) \mathcal{A}(\mathbf{q}, E, E + \hbar\omega). \quad (9.79)$$

Since

$$\langle G^R(\mathbf{x}, \mathbf{x}', E + \hbar\omega) G^A(\mathbf{x}', \mathbf{x}, E) \rangle = \frac{1}{V} \sum_{\mathbf{q}} e^{i\mathbf{q} \cdot (\mathbf{x} - \mathbf{x}')} \Phi(E, \mathbf{q}, \omega) \quad (9.80)$$

we obtain by using the spectral representation of the propagators, eq.(2.154), that

$$\Phi(E, \mathbf{q}, \omega) = \int_{-\infty}^{\infty} dE' \int_{-\infty}^{\infty} d\omega' \frac{N(E') \mathcal{A}(\mathbf{q}, E, E + \hbar\omega)}{(E + \hbar\omega - E' + i0)(E - E' - \hbar\omega' - i0)}. \quad (9.81)$$

We note that it follows from equation eq.(9.79) that at zero temperature

$$\mathcal{A}(\mathbf{q}, \epsilon_F, \epsilon_F + \hbar\omega) = -\frac{\Im m \chi(\mathbf{q}, \omega)}{\pi \omega N(\epsilon_F)}. \quad (9.82)$$

The term in the spectral correlation function, eq.(9.75), where $\lambda' = \lambda$ gives a delta function contribution, proportional to $\delta(\omega)$. In the case of extended wave functions the coefficient of the singular term vanishes in the thermodynamic limit, whereas from the region of energies where the states are localized we have a singular contribution.²¹ States which have equal energy, thus also have correlated wave functions. For the Fourier transform of the spectral correlation function we have

$$\mathcal{A}(\mathbf{q}, E, E + \hbar\omega) = A_E(\mathbf{q}) \delta(\omega) + A_E^r(\mathbf{q}, \omega) \quad (9.83)$$

where

$$A_E(\mathbf{x}) = \int \frac{d\mathbf{q}}{(2\pi)^d} e^{i\mathbf{q} \cdot \mathbf{x}} A_E(\mathbf{q}) = \frac{\hbar}{N(E)} \langle \sum_{\lambda} |\psi_{\lambda}(\mathbf{x})|^2 |\psi_{\lambda}(\mathbf{0})|^2 \delta(E - \epsilon_{\lambda}) \rangle \quad (9.84)$$

²¹This is the localization criterion of Berezinskii and Gor'kov [48].

and $A_E^r(\mathbf{q}, \omega)$ is a regular function vanishing at $\omega = 0$. We obtain from eq.(9.81) and eq.(9.83) the small ω behavior

$$\Phi(\mathbf{q}, \omega \rightarrow 0) \simeq \frac{2\pi N(E)}{-i\hbar\omega} A_E(\mathbf{q}). \quad (9.85)$$

In the insulating phase

$$\xi = \xi(E) \equiv \lim_{\omega \rightarrow 0} \sqrt{\frac{D(\omega)}{-i\omega}} \equiv \lim_{\omega \rightarrow 0} \xi(\omega) \quad (9.86)$$

is a positive constant, and the self-consistent theory gives

$$\Phi(E, \mathbf{q}, \omega) = \frac{2\pi N_0}{-i\hbar\omega} \frac{1}{1 + \xi^2 q^2} \quad (9.87)$$

or

$$A_E(\mathbf{q}) = \frac{1}{1 + \xi^2 q^2}. \quad (9.88)$$

According to eq.(9.84) we therefore find that the wave functions in a random potential are exponentially localized. In three dimensions, for example, we have

$$A_E(\mathbf{r}) = \frac{2\pi^2}{\xi^2 r} e^{-r/\xi} \quad (9.89)$$

and we identify ξ as the wave function localization length.

In two dimensions we obtain from eq.(9.73) for the wave function localization length within the self-consistent theory

$$\xi = \xi(\epsilon_F) = l e^{\frac{\pi k_F l}{2}}. \quad (9.90)$$

Exercise 9.3 Show that the localization length for a particle with energy E is determined by the expression

$$\xi^2(E) = \frac{1}{2dN(E)} \int d^d \mathbf{r} \mathbf{r}^2 \langle \sum_{\lambda} \delta(E - \epsilon_{\lambda}) |\psi_{\lambda}(\mathbf{x})|^2 |\psi_{\lambda}(\mathbf{0})|^2 \rangle. \quad (9.91)$$

Solution

The result follows from the sum-rule

$$\int d\omega \mathcal{A}(\mathbf{q}, E, E + \hbar\omega) = 1 \quad (9.92)$$

and the fact that in the small \mathbf{q} -limit, $\mathbf{q} \rightarrow \mathbf{0}$, we have

$$\mathcal{A}(\mathbf{q}, E, E + \hbar\omega) = (1 - \xi^2(E) \mathbf{q}^2) \delta(\omega) + \mathbf{q}^2 A_E^r(\omega). \quad (9.93)$$

Let us consider the localization length within the self-consistent theory in more detail. Multiplying both sides of eq.(9.70) with $\tilde{D}(\omega)/D_0$ yields

$$\begin{aligned} \frac{\tilde{D}(\omega)}{D_0} &= 1 - \frac{dk_F^{2-d}}{\pi k_F l} \int_0^{1/l} dQ \frac{Q^{d-1}}{-i\omega/\tilde{D}(\omega) + Q^2} \\ &= 1 - \frac{d}{\pi} \left(\frac{1}{k_F l} \right)^{d-1} \left(\frac{\xi(\omega)}{l} \right)^{2-d} \int_0^{\xi(\omega)/l} dx \frac{x^{d-1}}{1+x^2}. \end{aligned} \quad (9.94)$$

Since the diffusivity vanishes in the insulating phase we get the equation to determine the localization length

$$\begin{aligned} 1 &= \frac{dk_F^{2-d}}{\pi k_F l} \int_0^{1/l} dQ \frac{Q^{d-1}}{-i\omega/\tilde{D}(\omega) + Q^2} \\ &= 1 - \frac{d}{\pi} \left(\frac{1}{k_F l} \right)^{d-1} \left(\frac{\xi(\omega)}{l} \right)^{2-d} \int_0^{\xi(\omega)/l} dx \frac{x^{d-1}}{1+x^2}. \end{aligned} \quad (9.95)$$

In dimensions $0 < d < 2$ the integral converges for arbitrary $\xi = \xi(\omega = 0)$. In one dimension we get the localization length

$$\xi = 2.61 l \quad (9.96)$$

i.e., the localization length is of the order of the mean free path, in fair agreement with the exact result $\xi = 4l$ [39].

In two dimensions we get

$$\xi = \xi(\epsilon_F) = l \exp \left\{ \frac{1}{2} (\pi k_F l - 1) \right\} = \begin{cases} \exp \frac{\pi k_F l}{2} & k_F l \gg 1 \\ \sqrt{\pi k_F l} & k_F l \ll 1. \end{cases} \quad (9.97)$$

In the weak-disorder limit, $k_F l \gg 1$, the localization is exponentially weak in two dimensions, and experimentally weak-localization effects can easily be probed in two-dimensional systems, the subject of chapter 11. We note the nonanalytic dependence of the localization length on the disorder parameter $1/k_F l$.

The localization length calculated from the self-consistent theory agrees up to a numerical factor with the lowest-order perturbative estimate of section 9.2. This indicates that the higher-order terms in the scaling function, $1/g^n$, $n = 2, 3, \dots$ are small. In fact, Wegner has shown that the expansion starts out with a finite term of order $1/g^4$ [49].

9.3.4 Critical Exponents

In this section we will discuss the case where the spatial dimension is larger than two, $d > 2$, and the system can exhibit a metal-insulator transition. In dimensions larger than two, there always exists a solution of the self-consistent equation for

which the diffusivity at zero frequency is nonzero, $\tilde{D}(0) \neq 0$, provided the disorder parameter $\lambda \equiv \hbar/\pi p_F l$ is smaller than a certain critical disorder value λ_c . Using the identity

$$\frac{x^{d-1}}{1+x^2} = x^{d-3} \left[1 - \frac{1}{1+x^2} \right]$$

the expression eq.(9.94) can be rewritten as

$$\frac{\sigma(\omega)}{\sigma_0} = 1 - \frac{d}{d-2} \frac{1}{\pi} \left(\frac{1}{k_F l} \right)^{d-1} + \frac{d}{\pi} \left(\frac{1}{k_F l} \right)^{d-1} \int_0^{\xi(\omega)/l} dx \frac{x^{d-3}}{1+x^2}. \quad (9.98)$$

In the metallic phase, $\lambda < \lambda_c$, where $\xi(\omega \rightarrow 0) \rightarrow \infty$, the third term vanishes for all dimensions $d > 2$. In the limit of small ω we have

$$\frac{\sigma(0)}{\sigma_0} = 1 - \left(\frac{\lambda}{\lambda_c} \right)^{d-1} = C(\lambda/\lambda_c) \left(1 - \frac{\lambda}{\lambda_c} \right), \quad \lambda \leq \lambda_c \quad (9.99)$$

where $C(x) = \sum_{n=0}^{d-2} x^n$, and the critical value of disorder is identified as

$$\lambda_c = \left(\frac{d-2}{d\pi^{d-2}} \right)^{\frac{1}{d-1}}, \quad d \geq 2. \quad (9.100)$$

The dc conductivity vanishes at the critical disorder value $\lambda = \lambda_c$, and the transition is approached according to

$$\sigma(0) \propto \lambda_c - \lambda \quad (9.101)$$

i.e., with a critical exponent s for the conductivity equal to 1

$$\sigma(0) \propto |\lambda_c - \lambda|^s, \quad s = 1, \quad d > 2. \quad (9.102)$$

In the insulating regime, $\lambda > \lambda_c$, the dc conductivity vanishes, and eq.(9.98) determines the localization length

$$1 = \left(\frac{\lambda}{\lambda_c} \right)^{d-1} \left[1 - (d-2) \left(\frac{\xi}{l} \right)^{2-d} \int_0^{\xi/l} dx \frac{x^{d-3}}{1+x^2} \right]. \quad (9.103)$$

For dimensions $2 < d < 4$, the integral in eq.(9.103) converges as the localization length diverges, yielding a certain constant $c(d)$ depending on the dimension d . We are only interested in the scaling behavior of the localization length as the transition is approached, and there one has

$$\xi = c(d) l \left| 1 - \frac{\lambda}{\lambda_c} \right|^{\frac{1}{d-2}}, \quad c(d) = \left[2\pi \frac{d-1}{2-d} \sin \frac{\pi d}{2} \right]^{\frac{1}{d-2}} \quad (9.104)$$

i.e., the critical exponent ν for the localization length is $1/(d-2)$

$$\xi \propto |\lambda_c - \lambda|^{-\nu}, \quad \nu = \frac{1}{d-2}, \quad 2 < d < 4. \quad (9.105)$$

For dimensions larger than four, $d > 4$, one finds

$$1 = \left(\frac{\lambda}{\lambda_c}\right)^{d-1} \left[1 - \frac{d-2}{d-4} \left(\frac{\xi}{l}\right)^{-2}\right] \quad (9.106)$$

and thereby the scaling behavior

$$\xi \propto (\lambda - \lambda_c)^{-1/2}, \quad \lambda > \lambda_c \quad (9.107)$$

i.e., the critical exponent for the localization length is

$$\nu = \frac{1}{2}, \quad d > 4. \quad (9.108)$$

In dimensions $2 < d < 4$ the critical exponents satisfy the scaling relation

$$s = \nu(d-2), \quad 2 < d < 4. \quad (9.109)$$

which in three dimensions makes the two exponents identical, $\nu = s$.

The critical exponents were originally obtained by Wegner [36] employing the renormalization group in a field theoretic treatment of the disorder problem. Instead of studying the localization problem using diagrammatic perturbation theory, in this approach the impurity average is performed from the outset, and one is led to the field theoretic description of transport properties. For the impurity case one encounters the nonlinear σ model [36] [44]. The renormalization group technique can then be applied, thus making an interesting connection between quantum transport theory and the theory of phase transitions. The self-consistent theory of localization is the mean field approximation of the field theoretical model [47], and we have found that the critical dimension is $d = 2$, and the upper critical dimension is $d = 4$.

9.3.5 Scaling Behavior

The phenomenon of Anderson localization can be understood in terms of the random potential acting as a mirror backscattering the electronic wave function, thereby leading to a spatial localization of the particle.²² To probe the spatial localization we investigate the length-dependent scaling behavior. In a finite system there is a finite probability for a particle to reach the sample ends. As discussed in section 9.2, this influence on the conductivity is represented by a lower cutoff $1/L$ on the Q -integration. The diffusivity at zero frequency for a sample of length L , $\tilde{D}(L)$ is thus given by

$$\frac{\tilde{D}(L)}{D_0} = 1 - \frac{dk_F^{2-d}}{\pi k_F l} \int_{1/L}^{1/l} dQ \frac{Q^{d-1}}{\xi^{-2} + Q^2}. \quad (9.110)$$

²²In two dimensions even the slightest amount of disorder leads to localization, and the localization phenomenon is thus quite different from a localization due to the particle being in a bound state in a potential.

In the insulating phase, where $\tilde{D}(\omega = 0) = 0$, we have from eq.(9.94)

$$1 = \frac{dk_F^{2-d}}{\pi k_F l} \int_0^{\xi/l} dx \frac{x^{d-1}}{1+x^2}. \quad (9.111)$$

Subtracting eq.(9.111) from eq.(9.110) leads to

$$\frac{\tilde{D}(L)}{D_0} = \frac{d}{\pi k_F l} (k_F \xi)^{2-d} \int_0^{\xi/L} dx \frac{x^{d-1}}{1+x^2}. \quad (9.112)$$

Let us compute the current density J flowing in a sample of finite length L under the influence of the applied electric field E in, say, the x -direction. The current density J is determined by requiring it to be equal and opposite to the diffusion current under open-circuit conditions. The current density at the end of the sample is given by

$$J = -e\tilde{D}(L) \left. \frac{d(\delta n)}{dx} \right|_{x=L} \quad (9.113)$$

where $\delta n(x)$ is the electronic density change induced by the electric potential $U(x) = eE(L-x)$. The density change due to the external electric field is in linear response

$$\delta n(x) = \int_0^L dx' \chi(x-x') U(x'). \quad (9.114)$$

The density response function in eq.(9.114) is according to eq.(8.167) the Fourier transform of

$$\chi(\mathbf{q}, 0) = \frac{q^2}{\xi^{-2} + q^2} 2N_0 \quad (9.115)$$

and we obtain

$$\chi(x) = \int_{-\infty}^{+\infty} \frac{dq}{2\pi} e^{-iqx} \chi(\mathbf{q}, 0) = 2N_0 \left[\delta(x) - \frac{1}{2\xi} e^{-\frac{|x|}{\xi}} \right]. \quad (9.116)$$

For the current density we therefore have

$$J(L) = c_d e^2 E \xi^{2-d} \left(1 + \frac{L}{\xi}\right) \exp(-L/\xi) \int_0^{\xi/L} dx \frac{x^{d-1}}{1+x^2}, \quad (9.117)$$

where

$$c_d = \frac{2}{\pi} \frac{S_d}{(2\pi)^d} \quad (9.118)$$

and S_d is the surface area of the unit sphere in d dimensions.

For the dimensionless conductance we then obtain

$$g(L/\xi) = c_d (1 + L/\xi) e^{-L/\xi} h_d(L/\xi) \quad (9.119)$$

where we have introduced

$$h_d(y) = \int_0^1 dx \frac{x^{d-1}}{y^2 + x^2}. \quad (9.120)$$

In one and two dimensions we have²³

$$h_1(y) = \frac{1}{y} \arctan \frac{1}{y}, \quad h_2(y) = \frac{1}{2} \ln(1 + 1/y^2) \quad (9.121)$$

leading to

$$g(L) = \begin{cases} \frac{2\xi}{\pi^2 L} (1 + \frac{L}{\xi}) e^{-L/\xi} \arctan \xi/L & d = 1 \\ \frac{1}{2\pi^2} (1 + \frac{L}{\xi}) e^{-L/\xi} \ln \left(1 + \frac{\xi^2}{L^2}\right) & d = 2 \end{cases} \quad (9.122)$$

where ξ is the localization length given by eq.(9.104) for $\lambda < \lambda_c$. In the insulating regime, the conductance $g(L)$ decreases exponentially, and is negligibly small when the length of the sample is larger than the localization length ξ .

The self-consistent theory thus gives for the scaling function in the strong-disorder regime (in all dimensions)

$$\beta(g) = \ln g, \quad g \ll 1. \quad (9.123)$$

This was precisely the input we used in our discussion of the scaling theory of localization.

²³Note that for $d > 2$, $h_d(y) = \frac{1}{d-2} - y^2 h_{d-2}(y)$.

Chapter 10

Interactions in Metals

In this chapter we shall consider the interactions between the constituents of say a metal, i.e., electrons and ions. By adopting a mean field approach, the dynamics of the electrons can be obtained by perturbation theory from the properties of the noninteracting electrons, and the effective electron-electron interaction in good conductors is considered.¹ We shall not be interested in properties due to deviations from a spherical Fermi surface, and throughout we consider the isotropic model of a metal. The dynamics of the ions can for our purposes be treated in the harmonic approximation. In chapter 6 we introduced the formalism for describing a particle interacting linearly with oscillators without referring to the physical nature of the oscillators. As stipulated, this is a generic case which has wide applications. Indeed in this chapter, we shall give an account of the electron-phonon interaction, profiting from the results of chapter 6. In the case of phonons, the oscillators represent collective degrees of freedom, and we shall show how such an effective description comes about. We then calculate the collision rates due to electron-phonon and electron-electron interaction.

10.1 Isotropic Model of a Metal

A solid, such as a metal, is an assembly of nuclei and electrons. From a first principles point of view, the dynamics of such a system constitutes an unsolvable many-body problem as the number of involved particles is astronomical ($\sim 10^{23}$). We shall therefore be interested in an approximate description of the system, which is justifiable for the particular type of phenomena which is of our interest.

Electron diffraction or X-ray experiments reveal the grainy character of a metal. Charge is separated spatially into two pieces: the nuclei and the tightly bound electrons (core electrons which are concentrated in spatially well-localized regions), and the conduction electrons, which have their density spread throughout the solid. We are interested in the low-frequency dynamics, and can assume that the core electrons follow the motion of the nucleus adiabatically. The core electrons stay in

¹We shall use the words *metal* and *good conductor*, as applies to a heavily doped semiconductor, synonymously.